Precipitation monitoring in urban areas by a dense C-Band weather radar network

Laura Alku[1,4], Roberto Cremonini[1,2], Kalle Nordling[1] , Dmitri Moisseev[1,3]and V. Chandrasekar[1,3,4]

[1]*University of Helsinki, Department of Physics. Division of Atmospheric Sciences. Erik Palmenin Aukio 1 FIN-00014 University of Helsinki, Finland*
[2]*Agenzia Regionale per la Protezione Ambientale (ARPA) piemonte, Via Pio VII 9, 10135 Turin, Italy*
[3]*Finnish Meteorological Institute (FMI), Erik Palménin aukio 1, 00560 Helsinki, Finland*
[4]*Vaisala Oy, Vanha Nurmijärvetntie 21, 01670 Vantaa, Finland*
(Dated: 18th July 2014)

1 Introduction

High spatial and temporal resolution precipitation data is a crucial factor for hydrological applications in urban areas (Berndtsoon and Niemczynowicz, 1988). Small fluctuations in precipitation fields are of great importance considering the fast response of urban catchments due to the dominance of impervious surfaces. Hence, high resolution precipitation observations are needed in order to characterize these fluctuations. Several studies have been performed in order to provide recommendations on the temporal and spatial resolution of rainfall measurements required for hydrological applications in different climates (Schilling, 1991; Berne, 2004; Segond, ML et al, 2007).

Weather radars can provide high spatial and temporal resolution precipitation estimations. However, the quality of these observations in urban environments is significantly degraded by, among other things, ground clutter and beam-blockage. Data quality controls can be used to mitigate the effect of these challenges. Appropriate clutter techniques, scanning strategies and correction for attenuation might help to improve the quality of the observations. Nonetheless, there are areas where a single radar observation provides uncertain information about the precipitation echoes. Where feasible, a solution for this problem is weather radar networking, which makes it possible to fill one radars data gaps by using observations from others.

Very few cities have dedicated weather radar networks. In some cities, like Helsinki, there are several weather radars covering the metropolitan area, but they are operated by different organizations. The urban Helsinki area is covered by observations from three individual-purpose C-band polarimetric weather radars: Helsinki University's Kumpula (KUM), Vaisala Oy's Kerava (KER) and Finnish Meteorological Institute's Vantaa (VAN). Nonetheless, it is challenging to make them observe the same area at exactly the same time, which could lead to fast changing, short precipitation events being missed. Hence, synchronization and temporal resolution are the main concerns when building a network. In this study, we show how such systems can be used to build a network.

In order to decrease the impact of the synchronization and temporal resolution restrictions in the Helsinki radar network, we propose the use of the optic flow interpolation algorithm (Peura and Hohti, 2004) to retrieve information in between radar observations. In this method radar moments and the dual pol moments are retrieved by using the motion vectors calculated from the reflectivity fields. The retrieved dataset from the three radars is used to build radar composites which will be used to estimate rainfall using a combination of R(Z) and R(Kdp) relations for precipitation estimation.

2 Measurements

Helsinki area is densely monitored by three dual polarization C-band weather radars. Table 1 contains the specifications of the three systems. The average distance between these sensors is 16 km. Vantaa radar is located close to the international airport and is operated by the Finnish Meteorological institute. Kumpula radar is located in the Helsinki University Campus and serves as a research radar, located a few kilometers from downtown Helsinki. Kerava radar is located on top of the Kerava water tower approximately 23 km northeast of the city center. The topography of the area is flat and only few hills are present. Given this environment, typically 0.5 degree elevation PPI is quite free and close to the ground. Nevertheless, partial beam blockage occurs, especially for Kumpula and Vantaa radars, due to residential buildings and masts located close to the antennas. Figure 1 shows the locations of the three radars and the catchment areas where the precipitation estimation will be used.

The Kumpula and Kerava scanning strategy was modified to match the starting times of a dedicated precipitation monitoring task of the Vantaa radar couple of times per hour. The scans at the desired times consist of a PPI scan, single elevation of 1 degree for Kumpula and Kerava and volume scan for Vantaa at 1, 1.5 and 3 degrees of elevation. The measurements were set to pulse width of $2\,\mu s$, pulse repetition frequency of 570 Hz and maximum range of 100 km.

Figure 1:Helsinki radar network consist of three dual polarization C-band weather radars (KUM, KER and VAN). Within their observation area there are three small catchments (Pihlajanmäki, Pasila and Veräjämäki).

Table 1:Specifications of the three C-band weather radars of the Helsinki radar network .

	Helsinki radar networks systems		
	Kerava (KER)	Kumpula (KUM)	Vantaa (VAN)
Transmitter			
Type	Magnetron	Klystron	Magnetron
Operating frequency	5.5-5.7 GHz	5.610 GHz	5.5-5.7 GHz
Peak power	250kW	250kW	250kW
Pulse width	0.5, 0.8, 1.0, 2.0 µs	0.5 - 20.0 µs	0.5, 0.8, 1.0, 2.0 µs
PRF	200 to 2400 Hz	200 - 2000 Hz	200 to 2400 Hz
Antenna			
Type	Center-fed parabolic reflector	Center fed parabolic reflector	Center-fed parabolic reflector
Diameter	4.5 m	4.20 m	4.5 m
Gain (typical)	45 dB	~ 44.5 dB	45 dB
Beam width	<1 degree	1.05 deg	<1 degree
Peak on horizontal axis (typical)	-33 dB	-35 dB	-33 dB
RF-to-IF receiver			
Type	Dual stage, dual channel IF down converter	Dual stage, dual channel IF down converter	Dual stage, dual channel IF down converter
Dynamic range	> 99 dB (2 µs pulse) > 115 dB option	> 99 dB at 1 µs	> 99 dB (2 µs pulse) > 115 dB option
IF frequency	442/60 MHz	442 / 60 MHz	442/60 MHz
Pedestal			
Type	Semi yoke elevation over azimuth	Semi yoke elevation over azimuth	Semi yoke elevation over azimuth
Elevation range	-2 to 108 degrees	-2 to 108 degrees	-2 to 108 degrees
Maximum scan rate	40 deg/sec	40 deg/sec	40 deg/sec
Position accuracy	Better than 0.1 deg	Better than 0.1 deg	Better than 0.1 deg
Digital Receiver and Signal Processor			
Signal processor type	VAISALA SIGMET RVP900	VAISALA SIGMET RVP900	VAISALA SIGMET RVP900
IF digitizing	16 bits, 100 MHz in 5 channels	16 bits, 100 MHz in 5 channels	16 bits, 100 MHz in 5 channels

3 Methodology

The input of this approach corresponds to two consecutive dual-polarization observations from the dedicated task. Often residuals of ground clutter and other non-meteorological echoes remain in the observations, for this reason a simple post-processing filtering technique is applied to the radar images. After this data quality check, the images are used to retrieve

the information in between the two observations, using the optic flow algorithm proposed by Peura and Hohti in 2004. As a result reflectivity, Zh, and specific differential phase, KDP, fields are retrieved at 1 minute resolution. Subsequently, these fields are used to make composites, which at the final stage are used to create the network rainfall maps.

3.1 Data quality of radar observations using hydrometer classification filter

Attenuation due to the presence of the melting layer and beam blockage, presence of non-meteorological echoes and radar calibration are often, among other things, sources of bias when estimating precipitation. The use of signal processing algorithms, appropriate scanning strategies, and post processing corrections can be used to mitigate the impact of these undesired factors. As a starting point of this study non-meteorological echoes and calibration challenges were accounted for.

In order to reduce the impact of non-meteorological echoes on the radar observations a filter based on hydrometeor classification was applied. Figure 2 is an example of the filter effect on the input data for Vantaa radar observations on the 15th of July 2010 at 15:00 UTC. The Hydroclass^{TM} in the panel B of the figure 2 is the result of applying a filler filter over the raw Hydroclass^{TM} data in order to make it less noisy. The filler filter consists of a basic image processing technique which looks for the edges of the image and fills in the holes where thresholds have been applied. Using this data, a boolean map is created where the true entries correspond to meteorological data and the false values are the non-meteorological values. The boolean map is used to obtain only the meteorological echoes from the unfiltered reflectivity fields as in panel A in figure 2, resulting in less contaminated reflectivity fields as in panel C in figure 2. The same map is then applied over all the other radar variables.

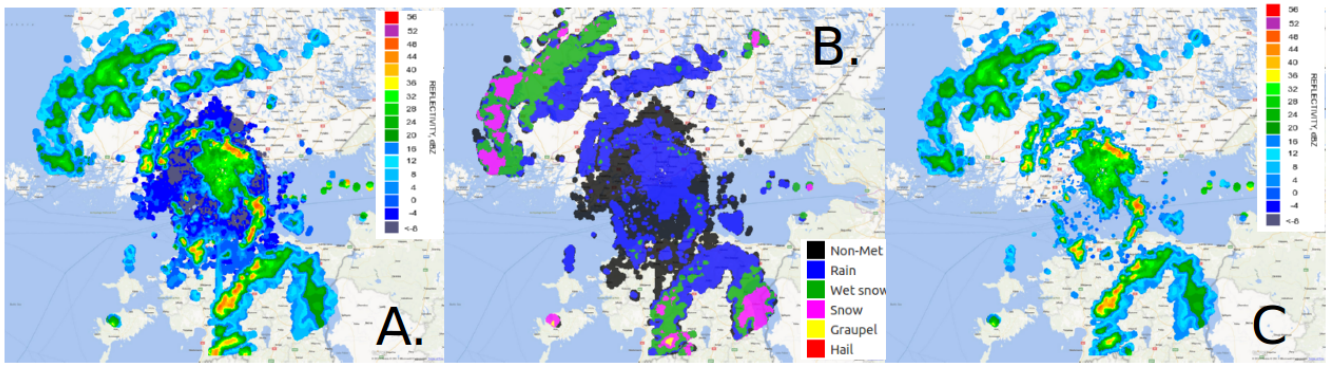

Figure 2: Hydroclass filter for Vantaa radar observations on the 15th of July 20101500 UTC. A. Unfiltered Reflectivity. B. Hydrometeor classification C. Filtered reflectivity

3.2 Interpolation of radar observations using optic flow algorithm

Figure 3 illustrates a general block diagram of the procedure of retrieving information between radar observations for increasing temporal resolution. The filtered fields of reflectivity are used to fill in the gaps existing between two observations. This retrieval is done by using the optic flow algorithm, which is a gradient based algorithm that assumes that the input are differentiable and that the changes are due to the motion (Proesmans, 1994; Bouguet J,2000). Under these assumptions, the motion vectors of the reflectivity fields are calculated and applied to interpolate all the radar variables.The interpolation for each variable is done forward (from observation at t=0 to the observation at $t=t^{+}$) and backwards (from observation at t=t to the observation at $t=t^{-}$) and the final output is the sum of both at time t.

The output images of the forward, I_1, and backward, I_2, interpolations at a time t, are defined by the equations 1.1 and 1.2 respectively. RV_i correspond to the radar variables' subsequent images and u and v are the magnitude and direction of the motion vectors of reflectivity.

$$I_1 = RV_1(x+tu, y+tv) \qquad (1.1)$$

$$I_2 = RV_2(x+(1-t)u, y+(1-t)v \qquad (1.2)$$

The resulting image M at time t is given by equation 1.3

$$M = (1-t)I_1 + tI_2 \qquad (1.3)$$

It is important to mention that a new M image is created for every radar quantity at each desired step. In this study the step used was 1 minute.

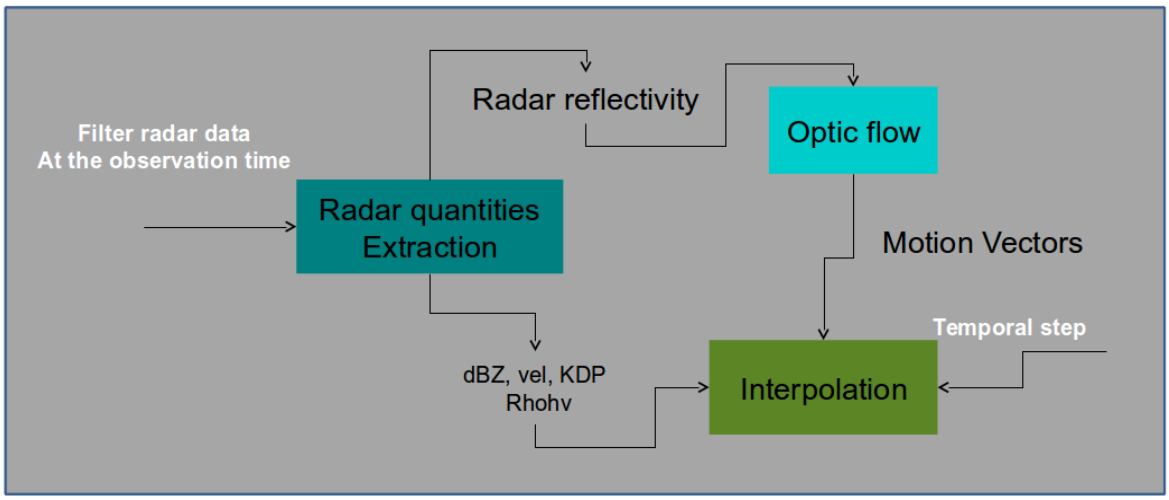

Figure 4: General block diagram of the interpolation procedure used to retrieve weather radar information in between two observations, based on the optic flow algorithm.

A preliminary evaluation of the performance of this approach over the dual pol quantities was attempted by comparing the retrieval KDP fields with the observations of the Vantaa radar. In this case we were only interested on the values of KDP greater than 0.2 degrees/km, which are going to be used for rainfall estimation adaptively when the reflectivity fields have values greater than a certain threshold as done by Ruzanski an Chandrasekar (2012). Figure 5 shows the scatter plot between the original observation from the Vantaa radar on the 8th of August 2010 at 17:35 UTC and both retrieved images when doing the interpolation procedure using 10 minute and 15 minute time difference between observations. From the picture we can see that there is an agreement between the retrieved values; the performance is better when using less time difference between observations. Further investigation is needed to evaluate in detail the performance of this approach over all the dual polarimetric variables.

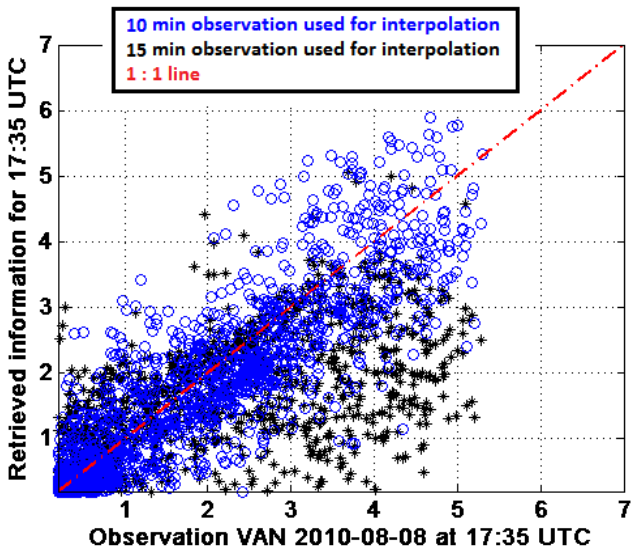

Figure 4: General block diagram of the interpolation procedure used to retrieve weather radar information in between two observations, based on the optic flow algorithm.

3.3 Radar Composites

Radar compositing has several advantages over single radar observations. Observations of single radars over areas where the topography of the region is challenging and data availability is limited -- due to for example aggressive clutter filtering or attenuation -- might have data gaps or negative bias. These gaps or bias can be replaced,where possible, by observations done by a second radar over the same area. There are multiple criteria when doing mosaicing of radar images. In this study we follow the maximum reflectivity principle for making the final image. Figure 6 shows in the top left panel the radar composite for the reflectivity field from observations of the Helsinki network radars of a convective storm on the 8th of August 2010 at 18:00 UTC. The top right panel corresponds to the Kumpula radar observation and on the bottom panel the observations from Kerava (left) and Vantaa (right) radars are shown.Vantaa and Kumpula observations present attenuation on the reflectivity

field on the left side of the moving front. Kerava, on the contrary, sees a high reflectivity cell in that area. The composite image allows recover that information from Kerava. However, also features like the secondary trip echoes seen by kumpula towards the north are part of the final image.

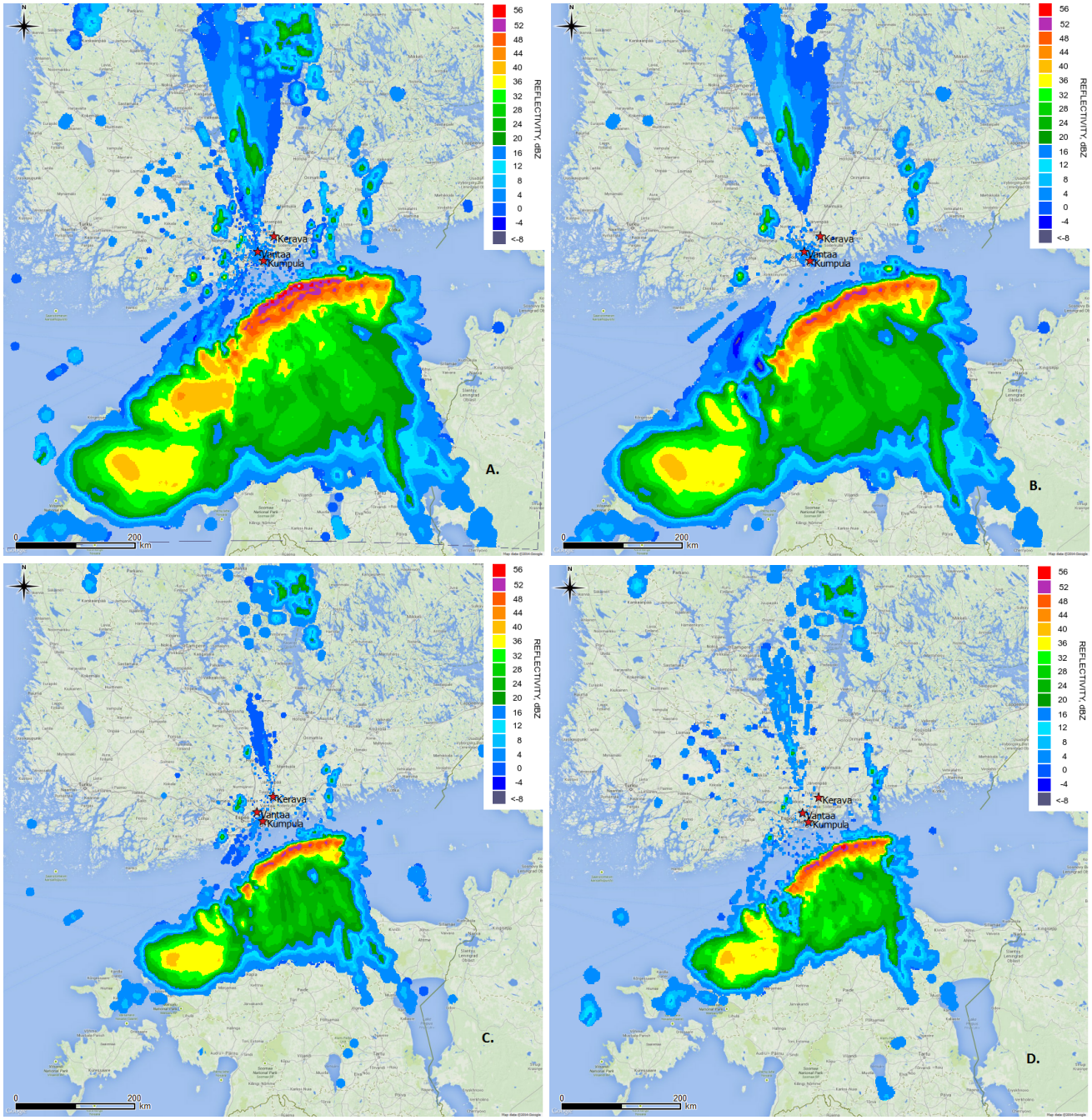

Figure 6: Radar reflectivity of a convective storm on the 8th of August 2010 18:00-18:15 UTC. A. Radar reflectivity composite. B. Radar reflectivity field from Kumpula. C. Radar reflectivity field from Kerava. D. Radar reflectivity field from Vantaa.

The calibration of the radar system on a network is an important factor when compositing images. When the systems are not calibrated during the measurement a post-processing correction technique can be applied. A common technique in satellite image elaboration is the relative radiometric correction. The main aim is to overcome the problem related to sensor miscalibration and atmospheric conditions. This technique is developed based on the assumption that there is a linear relationship between the digital numbers of co-located scenes. One of the most widely used methods is Histogram Matching (HM). This algorithm is used to match the histogram of one image to another. It uses the reference image histogram to modify the subject image histogram in order to make the second one similar to the reference image distribution (Xiaomin Yu et al., 2010). It is important to mention that for weather radar images the area over which this technique is applied should be smooth and must be the same geographic location for the images under use. The following figure shows an example of the HM

technique applied to Helsinki C-band weather radar on 5th October 2012 at 12 UTC. The Vantaa radar has been chosen as the reference.

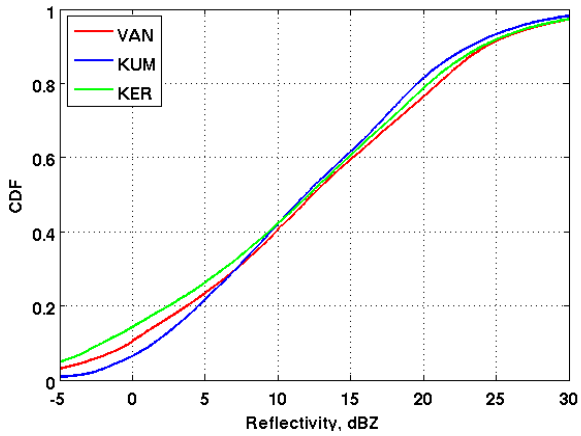

Figure 7: Histogram matching for Helsinki weather radar on the 5th October 2012 at 12 UTC.

3.5 Rainfall Estimation

The estimation of the rainfall field is the subsequent step after making the composites. At the end our goal is to provide the best estimation of precipitation with high temporal and spatial resolution. Standard Z-R relations have been determined depending on the climate, season and local conditions. However, with the dual-polarization variables the accuracy of the estimates has increased, because with them we have better information of the type and shape of the particles within the observation volume. Multiple relations using single or dual pol parameters or a combination of these with reflectivity have been established. A detailed description of these methods was done by Bringi and Chandrasekar (2001). For this preliminary study we used an adaptive rainfall estimation method as follows:

$$R(Z, KDP) = \begin{cases} 19\,KDP^{0.77} & KDP > \frac{1^o}{km} \text{ and } Z > 35dBZ \\ 316Z^{1.75} & Otherwise \end{cases} \qquad (1.4)$$

The coefficients used for the R(Z) relation are the ones that the Finnish meteorological institute uses for their doppler weather radar network (Saltikoff et al, 2010) when estimating rain. Figure 8 shows 1-hour accumulation in a convective storm on the 8th of August 2010 between 17:00-18:00 UTC calculated by the proposed adaptive R(KDP,Z) relation (bottom). We illustrate the effect of using the two parts of equation 1.4 over the whole precipitation field without any criterion. In the top right panel we can see that the second trip echoes (towards the North) from the Kumpula radar observations are enhanced by using the R(KDP) relation. Within the storm there were convective cells which by using the R(Z) relation (on the top left panel) are not visible. By using the adaptive R(KDP,Z) relation, we keep the details of the structure of the storm and avoid the overestimation of rainfall due to secondary trip echoes. An extensive validation of the results needs to be performed by running the methodology over different types of precipitation events and the coefficients for the R(KDP) relation need to be defined. The values we used in this preliminary estimation correspond to the values used by ARPA Piemonte.

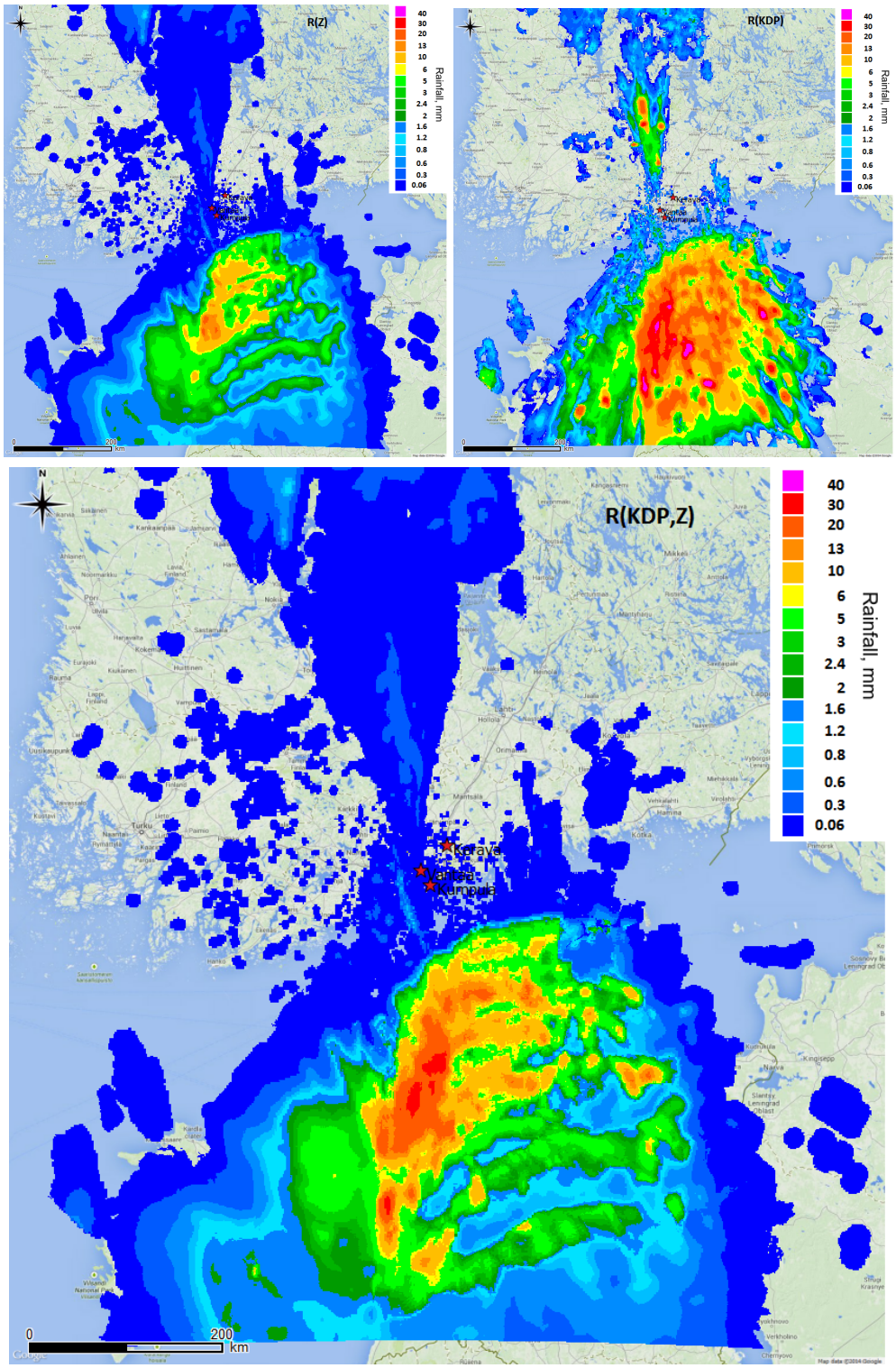

Figure 8: 1-hour accumulation in a convective storm on the 8th of August 2010 between 17:00 and 18:00 UTC calculated by: (bottom) adaptive R(KDP,Z) relation. (top-left) R(Z) relation and (top-right) R(KDP) relation.

4 Summary

In this study we built up a high resolution radar network for Helsinki urban area using three radars operated by different institutions. We noticed that even though the radars are operated by different institutions it is important that tasks with similar settings are scheduled at the radars as simultaneously as possible. Beam blockage, calibration and ground clutter will lead to biases when estimating rainfall. For this reason we propose here radar intercalibration and the hydrometer class based filter to address the latter two challenges. Radar intercalibration must be performed using the observations before building up

the composite to avoid biases in the result when max reflectivity criteria is used. The hydrometer class based filter must be applied to the radar observations before the interpolation, so that the initial and final observations are less contaminated with non-meteorological echoes.

An interpolation optic flow algorithm is proposed to increase the temporal resolution of radar observations. With this approach we aimed to retrieve radar variables in between subsequent observations using the reflectivity field motion vectors. After this radar reflectivity composites and maps of rainfall estimation were created. An adaptive rainfall R(Z,KDP) was presented as an option for precipitation estimation. However, the results presented in this study are preliminary results and an extensive validation using multiple cases needs to be performed, for both the adaptive rainfall estimation relations used and the performance of the interpolation procedure over the dual-polarization variables.

Acknowledgement

Support for this work was provided by TEKES CLEEN MMEA project, University of Helsinki and Academy of Finland (contract 263333).

References

Berndtsoon, R. and Niemczynowicz, J. Spatial and temporal scales in rainfall analysis - Some aspects and future perspectives // Journal of Hydrology. - July 1988. - 1-3 : Vol. 100. - pp. 293-313.

Schilling, W. Rainfall data for urban hydrology: what do we need? // Journal of atmospheric research.--December 1991.-1-3: Vol.27.-pp.5-21

Berne, A., Delrieu, G., Creutin, J. and Obled, C. Temporal and spatial resolution of rainfall measurements required for urban hydrology.// Journal of Hydrology,. December 2004, -1-3: Vol. 299. -pp. 166-179.

Segond, ML., Wheater, H. and Christian Onof, C. The significance of spatial rainfall representation for flood runoff estimation: A numerical evaluation based on the Lee catchment, UK // Journal of Hydrology. - December 2007.-1-2: Vol. 347.-pp. 116-131

Peura, M. and Hohti, H. Optic flow in radar images //Proceedings of ERAD. -2004-, - pp. 454–458.

Bouguet J., Pyramidal Implementation of the Lucas Kanade Feature Tracker: Description of the Algorithm, Technical report, OpenCV documents, Intel Corporation, Microprocessor Research Labs, 2000

Proesmans, M., Van Gool L., E. Pauwels E., and Oosterlinck A. Determination of optical flow and its discontinuities using non-linear diffusion // in 3rd European Conference on Computer Vision.- 1994-.-1: Vol. 2.-pp. 295–304.

Ruzanski, E. and Chandrasekar, V. Nowcasting Rainfall Fields Derived from Specific Differential Phase //J. Appl. Meteor. Climatol. -May 2012-. 1: vol. 51. -pp 1950–1959

Xiaomin, Y., Zhan, F.B., Jinxing H. and Qin Z. Radiometric normalization for multitemporal and multispectral high resolution satellite images using ordinal conversion // 18th International Conference on Geoinformatics. -June 2010- 4: Vol.1-pp18-20

Bringi, V. N. and Chandrasekhar, V. Polarimetric Doppler Weather Radar. Principles and Applications//Cambridge University Press, -NY 2001-,-pp 636.

Saltikoff, E. Huuskonen, A. Hohti, H., Koistinen, J. and Järvinen, H. Quality assurance in the FMI Doppler Weather Radar Network. //Boreal environment research.-December 2010-. 1: Vol: 15.-pp 579-594.